Geotechnical Aspects of Underground Construction in Soft Ground – Ng, Huang & Liu (eds)
© 2009 Taylor & Francis Group, London, ISBN 978-0-415-48475-6

Characteristics of tunneling-induced ground settlement in groundwater drawdown environment

C. Yoo & S.B. Kim
Sungkyunkwan University, Suwon, Korea

Y.J. Lee
RIST, Yongin, Korea

ABSTRACT: This paper presents the results of an investigation on the characteristics of tunnelling-induced ground settlement in groundwater drawdown environment. The dynamics of the effect of groundwater drawdown on the ground settlements are first investigated using a case history concerning a conventional tunnelling situation in which the interaction between the tunnelling and the groundwater induced excessive ground surface settlements. A 2D stress-pore pressure coupled finite element analysis is then conducted on a tunnelling case with groundwater drawdown, aiming at investigating ground surface settlement characteristics. The results indicated among other things that significant portion of ground settlement can occur before tunnel face reaches, and that the error function approach does not provide a good fit to the settlement troughs for tunnelling cases with groundwater drawdown.

1 INTRODUCTION

Tunnelling beneath the groundwater table causes changes in the state of stress and the pore water pressure distribution. In such tunnelling problems, the tunnelling work inevitably causes water inflows into excavated area, thus causing the change in the pore water pressure distribution. The direct environmental consequence of water inflows during tunnelling is the drawdown of groundwater level in the surrounding aquifer (Yoo 2005). The related ground subsidence occurring as a result of the reduction in water pressures in the soil layers can damage nearby structures/utilities (Figure 1). One of the major case histories illustrating damage due to ground settlement associated with tunneling-induced groundwater drawn is perhaps the Romeriksporten tunnel in which the highspeed railway tunnel construction caused more 1 m of ground subsidence due to groundwater drawdown, raising significant technical and political issues pertaining to the effect of tunnelling on surrounding environment (NSREA 1995).

Surprisingly studies concerned with the tunneling-induced ground movements in groundwater drawdown are scarce as indicated by Yoo (2005). Although a number of studies on the ground subsidence caused by groundwater pumping from an aquifer have been conducted (Shen et al. 2006; Qiao & Liu 2006; Xu et al. 2006). The results of their studies cannot be directly applied to the tunnel excavation problems as they focused only on the groundwater drawdown due to groundwater pumping. As urban tunnelling projects tend to involve potential problems related to groundwater drawdown ground movements during tunnelling, there is an urgent need for better understanding on the mechanisms involved in tunnelling-induced ground movements associated with groundwater drawdown.

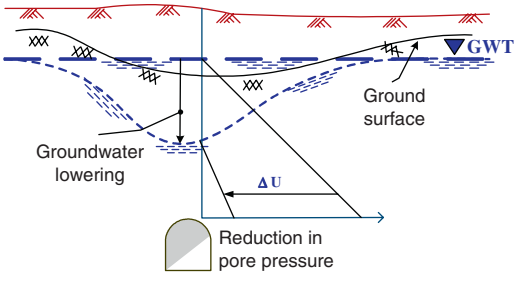

Figure 1. Illustration of ground settlement associated with tunnelling-induced groundwater drawdown.

This paper presents the results of investigation on the characteristics of tunnelling-induced ground settlement in groundwater drawdown environment. The

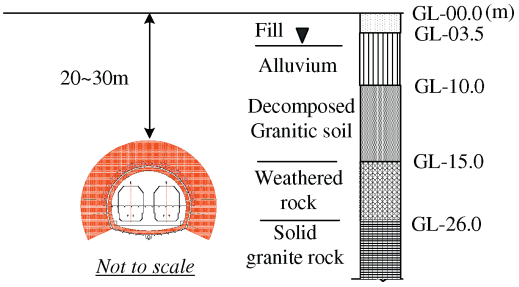

Figure 2. Typical ground profile.

Table 1. Geotechnical properties of soil/rock layers.

Type	γ (kN/m^3)	c' (kPa)	ϕ' (deg)	E (MPa)	ν	k (cm/sec)
fill	18	0	27	5	0.40	3.8×10^{-4}
alluvial	20	15	30	10	0.40	3.8×10^{-4}
weathered soil	25	15	30	50	0.33	2.4×10^{-4}
weathered rock	25	60	35	120	0.30	8.8×10^{-5}
hard rock	26	100	35	200	0.25	5.0×10^{-5}

Note: γ = unit weight, c' = cohesion, ϕ = internal friction angle, E = young's modulus, ν = poisson's ratio, K = coefficient of permeability

dynamics of the effect of groundwater drawdown on the ground settlements are first investigated using a case history concerning a conventional tunnelling situation in which the interaction between the tunnelling and the groundwater induced excessive ground surface settlements. A parametric study using a calibrated 2D stress-pore pressure coupled finite element model is then conducted on a number of factors influencing the tunnelling-induced ground settlements with groundwater drawdown. Based on the results, the interaction mechanism between the tunneling, groundwater lowering, and ground settlement is identified.

2 GROUND SURFACE SETTLEMENT CHARACTERISTICS – FIELD MONITORING DATA

2.1 *Tunnelling condition*

A case history concerning the conventional tunnelling, i.e., NATM, was considered. The tunnel has excavation width and height of approximately 10.5 m and 8.7 m, respectively, with a cover depth ranging approximately 20 ~ 30 m, and constructed in a multi-layered ground including a fill, alluvium, and a weathered zone as illustrated in Figure 2. The geotechnical properties of the ground are given in Table 1.

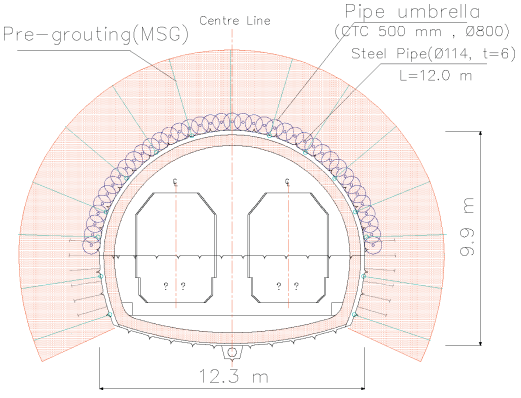

Figure 3. Support pattern (typical).

2.2 *Tunnel design*

Figure 3 shows a typical tunnel support pattern used for a 100 m long section for the ground profile given in Figure 2. On account of the difficult ground condition the ring cut excavation method was adopted to promote the tunnel face stability during excavation. The primary support system consisted of a 0.2 m thick steel fibre reinforced shotcrete (SFRS) layer with 4 m long system rock bolts at 1.0 and 1.2 m, respectively, longitudinal and transverse spacing. The pipe umbrella technique using 800 mm diameter grout injected 12 m long steel pipes was additionally implemented to promote the face stability through improving the load carrying capacity of the ground ahead of the face. Also adopted was a trumphet shaped micro cement injection (MSG) pre-grouting around the tunnel periphery to create a 5 m thick watertight shell for sections in which the weathered soil layer extended to the tunnel crown level. The pre-grouting scheme was later extended to cover the face after the settlement problem had become an issue.

2.3 *Measured ground surface settlements*

Figure 4 shows the progressive development of settlements during the tunnel advancement at various monitoring stations. In this figure the measured settlements are plotted against the relative distance between the tunnel face and the monitoring stations normalized by the tunnel diameter (D). These data, measured using the conventional leveling technique, thus indeed represent the settlement history during the tunneling process for the monitoring stations.

A total of five settlement curves are presented in this figure. As can be seen in this figure the five curves are similar both in qualitative and quantitative terms, despite the vertical extent of the decomposed soil relative to the tunnel varies along the route, showing the maximum converged settlements in the range of

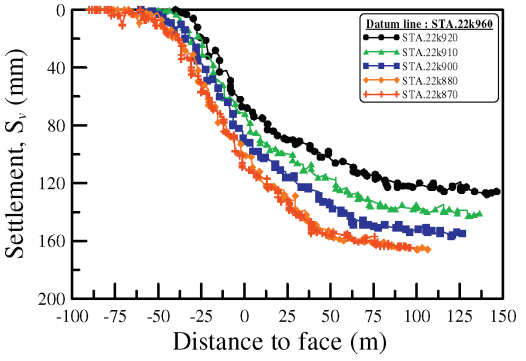

Figure 4. Progressive development surface settlements at various monitoring stations.

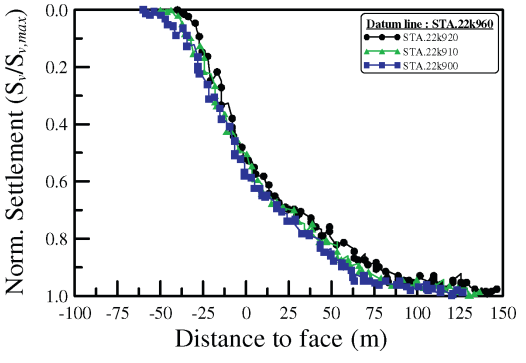

Figure 5. Normalized settlement history curves.

1.6% ~ 1.8%D. Of salient feature that can be observed in this figure is the tendency of settlement increase during which the tunnel advancement was halted, suggesting time dependent (tunneling activity independent) settlement development (to be discussed later). Another of interest trend is the resemblance of the settlement curves with a typical log **t** curve from a consolidation test, being characterized by three zones as an initial compression, primary, and a secondary zone. Such a trend strongly suggests a possible cause being the volume change effect due to tunneling-induced groundwater drawdown.

The data in Figure 4 are further analyzed by normalizing the settlement values with their respective maximum values ($S_{v,max}$) in Figure 5. As seen in this figure, the normalized curves tend to collapse into one curve. A further inspection of the normalized settlement history curves shows that the settlements started to develop when the tunnel face was approximately 6D away from the monitoring stations. The settlements tend to accelerate when the tunnel face reached 3D away from the monitoring stations, and decelerate after the tunnel advanced 5 ~ 6D beyond the monitoring stations. Also shown are that approximately 60 ~ 70% of the final settlement ($S_{v,max}$) was completed before the face passed a monitoring station with the remaining 30 ~ 40% occurred after the full passage of the tunnel face. Such a percentage of settlement ahead of the face is considerably larger than the typical value of 40 ~ 50%, suggesting a larger portion of the converged settlement occurred prior to the arrival of tunnel face in this tunneling condition than a tunneling condition without the groundwater drawdown. Moreover, the settlements tend to converge to a constant value after the tunnel face advanced to a distance of 6 ~ 7D beyond the monitoring stations, suggesting slower settlement convergence than a normal condition.

These results in fact are somewhat different from typical trends that can be observed in tunneling conditions without significant groundwater lowering, and led to a conclusion that factors other than the unloading effect due to the tunnel excavation may have played a role. Such a tendency is directly linked to the groundwater drawdown as will be shown in a subsequent chapter.

3 PARAMETRIC STUDY

3.1 *Stress-pore pressure coupled analysis*

A commercial finite element package ABAQUS (Abaqus, Inc. 2002) was used for the parametric study. A 2D stress-pore pressure coupled effective formulation was adopted in order to realistically capture the interaction mechanism between the tunnelling and the groundwater.

In ABAQUS a porous medium is approximately modelled by attaching the finite element mesh to the solid phase. Equilibrium is expressed by writing the principle of virtual work for the volume under consideration in its current configuration at time t:

$$\int_V \boldsymbol{\sigma} : \delta\boldsymbol{\varepsilon}\, dV = \int_S \mathbf{t}\cdot\delta\mathbf{v}\, dS + \int_V \hat{\mathbf{f}}\cdot\delta\mathbf{v}\, dV \tag{1}$$

where dv is a virtual velocity field, $d\varepsilon$ is the virtual rate of deformation, σ is the true (Cauchy) stress, t are surface tractions per unit area, and **f** body forces per unit volume. **f** includes the weight of the wetting liquid $\mathbf{f_w}$ defined as Eq. (2)

$$\mathbf{f}_w = (sn + n_t)\rho_w\, \mathbf{g} \tag{2}$$

in which s is the degree of saturation, n is the porosity, and n_t is the volume of trapped wetting liquid per unit of current volume. Eq. (1) can then be rewritten as

$$\int_V \boldsymbol{\sigma} : \delta\boldsymbol{\varepsilon}\, dV = \int_S \mathbf{t}\cdot\delta\mathbf{v}\, dS + \int_V \mathbf{f}\cdot\delta\mathbf{v}\, dV + \int_V (sn + n_t)\rho_w\mathbf{g}\cdot\delta\mathbf{v}\, dV \tag{3}$$

Table 2. Geotechnical properties.

	γ (kN/m^3)	E (kPa)	c (kPa)	ϕ (°)	k (cm/sec)
soil	25	50,000	30	30	5.8×10^{-3}
Weathered rock	25	100,000	50	30	1.3×10^{-4}

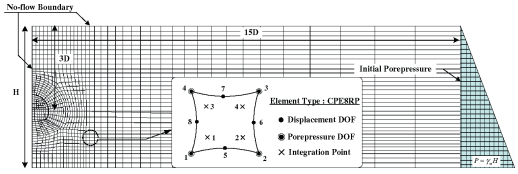

Figure 6. Finite-element model used in the analysis.

where **f** are all body forces except the weight of the wetting liquid.

The continuity equation is satisfied approximately in the finite element model by using excess wetting liquid pressure as the nodal variable (degree of freedom 8), interpolated over the elements. The backward Euler approximation is used to integrate the equation over time and the Newton iterations are used to solve the nonlinear, coupled, equilibrium and continuity equations. Fundamentals of the stress-pore pressure coupled formulation adopted in ABAQUS can be found in the ABAQUS user's manual (Abaqus, Inc. 2005).

3.2 *Condition analyzed*

A tunnelling condition frequently encountered in urban situations was considered in the analysis. The tunnel considered is a 10 m diameter horseshoe shaped tunnel with a cover depth of 3.0D, excavated by the bench cut method. The primary support system consists of a 20 cm thick shotcrete lining with system rock bolts installed at 1.5 m center-to-center spacing. A 1.5D thick soil layer was assumed to exist above a weathered rock layer through which the tunnel is excavated. Tables 2 summarizes geotechnical properties of the ground.

3.3 *Finite element model*

Figure 6 shows the finite element model adopted in this study. The finite-element mesh extends to a depth of two times the tunnel diameter (D) below the tunnel spring line and laterally to a distance of 15D from the tunnel center depending on the cover depth H. The lateral location was selected based on a series of preliminary analysis as it has a significant influence on the results of a stress-pore pressure coupled analysis. At the lateral boundary displacements perpendicular to the boundaries were restrained whereas pin supports were applied to the bottom boundary.

With regard to the hydraulic boundary conditions and with reference to Figure 6, a no-flow condition was assigned to the vertical boundaries perpendicular to the tunnel drive. At the lateral vertical boundary the groundwater table was assumed to be at the ground surface and constant throughout the analysis.

The ground and the shotcrete lining were discretized using 8-node displacement and pore pressure elements with reduced integration (CPE8RP). The rock bolts were modeled using the 2-node truss elements. With regard to the material modelling, the soil and rock layers were assumed to be an elasto-plastic material conforming to the Mohr-Coulomb failure criterion together with the nonassociated flow rule proposed by Davis (1968), while the shotcrete lining and the rock bolts were assumed to behave in a linear elastic manner. The geotechnical properties for the ground given in Table 1 were used for analysis. The young's moduli of the shotcrete and rock bolts were chosen as 15 GPa and 21 GPa, respectively.

The actual tunnelling process consisting of a series of excavation and support installation stages was closely simulated in the analysis by adding and removing corresponding elements at designated steps. After establishing the initial stress and pore pressure conditions with appropriate boundary conditions, the step-by-step tunnelling process pertinent to the bench cut excavation method, was then simulated. The 3D effects of advancing a tunnel heading was taken into consideration using the stress relaxation method in which the boundary stresses arising from the removal of excavated elements are progressively applied to simulate the progressive release of the excavation forces as the tunnel heading advances.

3.4 *Ground settlement characteristics*

Figure 7 presents the relationship between the maximum surface settlement ($S_{v,\max}$), directly above the tunnel crown, obtained during various stages of tunneling. As seen the maximum surface settlement $S_{v,\max}$ tends to linearly increase with the increase in the groundwater drawdown level H_D. The settlement occurred after the completion of tunnel is in fact twice that during the tunnel excavation. It should be noted that the plot given in this figure represent those caused by the groundwater inflow into the tunnel after the completion of tunnel excavation, until a steady state condition is achieved. This suggests a direct link between the ground settlement and the groundwater drawdown, thus demonstrating the importance of creating a watertight shell for tunnelling cases where the controlling ground surface settlement is of concern.

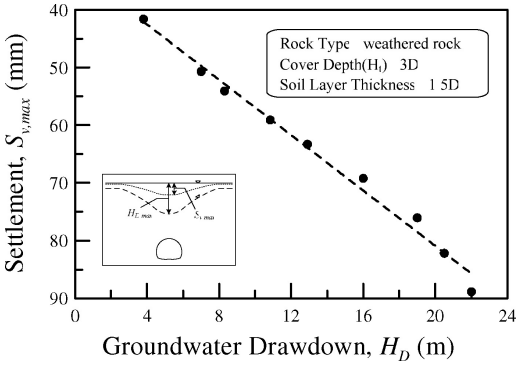

Figure 7. Variation of $S_{v,\max}$ with H_D after completion of tunnel excavation.

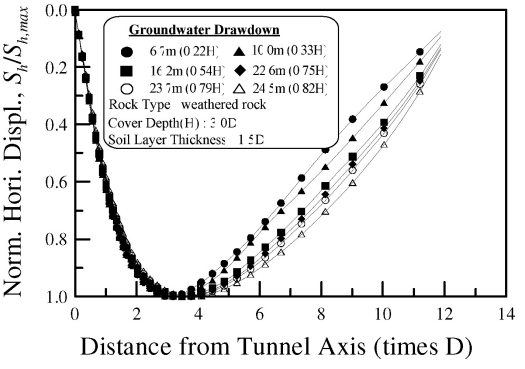

Figure 9. Normalized surface horizontal displacement profiles.

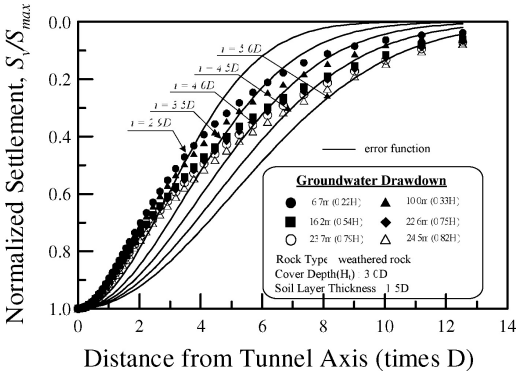

Figure 8. Normalized surface settlement troughs.

In urban tunnelling situations, characteristics of a ground surface settlement trough, such as slope and width of inflection point, are important as they, together with lateral displacements, determine potential for damage of adjacent structures. Figure 8 shows normalized ground surface settlement troughs for different groundwater drawdown levels together with error functions constructed using different values of inflection point. Of interest trends are two fold. First, the extent of ground settlement trough is significantly greater than typical tunnelling conditions without groundwater drawdown. In fact, for the particular tunnelling condition considered, the ground settlement zone extends more than 10 times the tunnel diameter from the tunnel centerline. Second, the error function approach (Attewell et al. 1986; Peck 1969) known to well describe the surface settlement trough for tunnelling cases without ground water drawdown does not provide a good fit to the settlement troughs for cases with groundwater drawdown. Another important observation is that the computed settlement troughs tend to collapse into one curve despite some discrepancies in the region father away, i.e., $\geq 4D$, from the tunnel center.

Normalized horizontal displacement (S_h) profiles are shown in Figure 9 for different levels of groundwater drawdown. As seen, the maximum horizontal displacements ($S_{h,\max}$) tend to develop at locations 3D away from the tunnel center with decreases in magnitudes thereafter. Again the S_h profiles tend to collapse into one curve although some discrepancies are observed in the region away from the tunnel center. The results obtained in this study suggest that the settlement trough as well as the horizontal displacement profile may be constructed using normalized curves when relationships between the surface movements and other factors can be established.

4 CONCLUSIONS

This paper presents the results of an investigation on the characteristics of tunnelling-induced ground settlement in groundwater drawdown environment using the measured surface settlement for a site where the tunnelling-induced groundwater drawdown caused significant surface settlement. A stress-pore pressure coupled finite element model was additionally conducted aiming at identifying the ground movement characteristics when tunnelling induces a significant level of groundwater drawdown. Based on the results the following conclusions can be drawn.

1. For tunnelling cases in which tunnel excavation causes significant groundwater drawdown, the percentage of settlement that develop prior to the tunnel face arrival to the final settlement is significantly larger than for cases without groundwater drawdown.

2. Continued groundwater drawdown after the completion of tunnel excavation may can cause settlement larger than that occur during excavation.
3. The error function does not provide a good fit to the settlement troughs for cases with groundwater drawdown.
4. Normalization can hold for the surface settlement and horizontal displacement profiles for tunnelling cases with groundwater drawdown.

ACKNOWLEDGEMENT

This research is supported by Korea Ministry of Construction and Transportation under Grant No. C4-01. The financial support is gratefully acknowledged.

REFERENCES

Abaqus users manual, Version 6.5. 2005. Hibbitt, Karlsson, and Sorensen, Inc., Pawtucket, Providence, R.I.

Attewell, P.B., Yeates, J. & Selby, A.R. 1986. Ground deformation and strain equations. *Soil movements induced by tunneling and their effects on pipeline and structures*, Blackie, Glasgow: 53–66.

Norwegian Soil and Rock Engineering Association (NSREA). 1995. *Norwegian urban tunnelling*. Publication No. 10., Norway.

Peck, R.B. 1969. Deep excavations and tunneling in soft ground *Proc., 7th Int. Conf. on Soil Mech. And Found. Engrg*. : 225–290.

Qiao, S. & Liu, B. 2006. Prediction of ground displacement and deformation induced by dewatering of groundwater. *Underground Construction and Ground Movement*: 73–79.

Shen, S.L., Tang C.P., Bai, Y. & Xu, Y.S. 2006. Analysis of settlement due to withdrawal of groundwater around an unexcavated foundation pit. *Underground Construction and Ground Movement*: 377–384.

Xu, Y.S., Shen, S.L. & Bai, Y. 2006. State-of-art of land subsidence prediction due to Groundwater Withdrawal in China. *Underground Construction and Ground Movement*: 58–65.

Yoo, C. 2005. Interaction between Tunnelling and Groundwater-Numerical Investigation Using Three Dimensional Stress-Pore Pressure Coupled Analysis. *Journal of Geotechnical and Geoenvironmental Engineering, ASCE* 131(2): 240–250.